

Ya-Jong Zhang

international
**ELECTRON
DEVICES**
meeting

1990

SAN FRANCISCO, CA
DECEMBER 9-12, 1990

TECHNICAL DIGEST

2001



Sponsored by Electron Devices Society of IEEE

TECHNICAL DIGEST

ieeem

BASE TRANSPORT IN NEAR-IDEAL GRADED-BASE Si/Si_{1-x}Ge_x/Si HETEROJUNCTION BIPOLAR TRANSISTORS FROM 150 K TO 370 K

E.J. Prinz and J.C. Sturm

Department of Electrical Engineering, Princeton University,
Princeton, NJ 08544 (609-258-6624)

Abstract

In this paper we present a detailed study of electron base transport in Si/Si_{1-x}Ge_x/Si graded-base npn heterojunction bipolar transistors. The temperature dependence from 150 to 370 K of the collector current in near-ideal devices with various base gradings is examined, and it is shown that this collector current can be modelled over the entire temperature range by a simple analytical formula. Also, graded base devices with an estimated room temperature base spreading resistance of 7KΩ/□ have a gain of about 4000 at 89K.

Introduction

Si/Si_{1-x}Ge_x/Si heterojunction bipolar transistors (HBT's) are promising candidates for high speed circuitry. While initial devices had flat germanium profiles across the base, recent work has focussed on devices with graded Ge profiles to provide a built-in field to aid the electron transport. Room-temperature performance of 75 GHz¹ has been reported in these structures. In this paper an analytical model for the base transport of electrons in these devices will be presented and experimentally confirmed. Further, the near-ideal base currents in these devices yield very high current gains, even at 89K.

Theoretical Description

It is well known that the DC collector current of Si/SiGe/Si npn HBT's with a flat germanium profile in the base can be modelled by applying a factor $\exp(-\Delta E_V/k_B T)$ to the basic Gummel-Poon model of silicon devices, where ΔE_V is the valence band offset between silicon and the strained SiGe. A model for devices with varying amounts of germanium across the base can be developed by realizing that p-type SiGe with doping N_A and p-type Si with doping $N_A \cdot \exp(-\Delta E_G/k_B T)$ have the same conduction band position with respect to the Fermi level (Fig. 1), where ΔE_G is the difference between the bandgaps of Si and the SiGe. Since this conduction band position determines the electron transport across the base, a SiGe device can be transformed into an "effective" silicon device which would have the same current of electrons across the base. Using the conventional Gummel

number approach to model the current in the effective Si device, an effective Gummel number, $N_{G,eff}$, can be calculated for the SiGe device.³ While this formalism can be applied to arbitrary base profiles, in the case of a base which is graded linearly in germanium concentration and with constant doping (Fig. 2), $N_{G,eff}$ can be evaluated analytically:

$$N_{G,eff} = \int_0^W N_A(x) e^{\frac{-\Delta E_G(x)}{k_B T}} dx$$

$$= \frac{W N_A k_B T}{\Delta E_{G,2} - \Delta E_{G,1}} e^{-\frac{\Delta E_{G,1}}{k_B T}} \left(1 - e^{-\frac{\Delta E_{G,2} - \Delta E_{G,1}}{k_B T}} \right) \quad (1)$$

where $\Delta E_{G,1}$ and $\Delta E_{G,2}$ are the minimum and maximum bandgap differences respectively, W is the neutral base width, and N_A the constant base doping concentration. Based on this formula, the predicted ratio of collector current for SiGe devices to Si devices for the graded structures of Fig. 3 devices is shown in Fig. 4. (Differences in densities of states and diffusion constants between the SiGe and Si have been ignored). One notes that since the grading of our structures was always sufficiently large, the term in parentheses in (1) is always close to unity. Therefore the temperature dependence of the current enhancement from one device to another depends only on $\Delta E_{G,1}$, i.e., the barrier for electrons at the emitter side of the base (Fig. 2).

Device Fabrication

The graded HBT structures of Fig. 3 were grown by rapid thermal chemical vapor deposition in a lamp heated system. Emitter and collector dopings were $\sim 5 \times 10^{17} \text{ cm}^{-3}$, the targeted base dopings were $\sim 5 \times 10^{18} \text{ cm}^{-3}$, and the base widths were 500Å. The collector layers were grown at $\sim 1000^\circ \text{C}$, the base layers from 625 to 700°C, and the emitter layers at 850°C. The wafer was not cooled to room temperature between the growth of the individual layers as in Limited Reaction Processing⁴, but the wafer temperature was changed directly from the condition for one layer to that for the next. Transistors were then fabricated using a planar process. Individual devices were isolated by plasma-etched mesas. Base contact was established by boron implants. To improve the emitter contact, a

shallow arsenic implant was used. The devices were passivated with a SiO₂ film deposited by plasma deposition at 350 °C. The implants were then annealed for 10 minutes at 800 °C. Titanium/aluminum metallization and patterning completed the processing.

Experimental Results and Discussion

Typical room-temperature Gummel plots and common-emitter characteristics are shown in Fig's. 5 and 6. Note that the collector current is enhanced in devices with more germanium. This can be understood physically by the reduced barrier in the base that electrons must overcome on their way from emitter to collector (Fig. 2). The base current slope is near-ideal ($\sim 62\text{mV/decade}$). This indicates that the base current probably results from neutral base recombination or from injection of holes into the emitter. Since the base currents are virtually identical for all devices despite the different base profiles, we conclude that the base current is dominated by hole injection into the emitter; this is because the valence band barrier for holes from base to emitter is the same in all devices, independent of the Ge profile in the base (see Fig. 2). The 13-20% device had a room temperature current gain of ~ 1000 . The emitter collector breakdown voltage was only $\sim 2\text{ V}$ in all devices, but this is consistent with the collector doping of $\sim 5 \times 10^{17}\text{ cm}^{-3}$.

Temperature dependent measurements of the collector current enhancement are shown in Fig. 7, along with the predictions of the model, using the structure parameters of Fig. 3, and the bandgaps for strained SiGe from Ref. 5. Because of the high base doping compared to that of the emitter and collector, depletion into the base layer is negligible, and thus the Ge concentrations at the edge of the neutral base should not differ significantly from the Ge concentrations at the extreme edges of the SiGe layers. Therefore the germanium limits of Fig. 3 were used directly in Eqn. (1) for the predictions. The agreement of the model with the experimental data is good considering that no adjustable parameters were used. Except for the device with no germanium at the emitter side of the base, the model always slightly overestimates the temperature dependence of the current enhancement. Part of this overestimation may be due to the neglect in the simple model presented here of the effect of density of states differences between Si and strained SiGe, and part is probably due to uncertainties in the Ge percentages ($\sim 2\%$). Fitting the model parameters to the data also shows that some devices have Gummel numbers less than targeted; a best fit for 13-20% Ge device (#3) yields a Gummel number of $1 \times 10^{13}\text{ cm}^{-2}$ instead of $2.5 \times 10^{13}\text{ cm}^{-2}$.

Typical low-temperature performance (Gummel plots) of two devices is shown in Fig. 8 (201 K).

Because the effect of the narrow bandgap base more than compensates for the effects of bandgap narrowing in the heavily doped emitter contact, the gain of the devices with larger amounts of Ge in the base actually improves at lower temperature. The temperature dependence of the maximum current gain of devices #1 and #3 is shown in Fig. 9. Structure #1 (0 - 20% Ge) has a gain that is roughly independent of temperature, and structure #3 (13-20% Ge) has a gain that actually rises as the temperature is decreased, reaching a maximum value of 4000 at 89K. This device is estimated to have a room temperature base spreading resistance of only $\sim 7\text{K}\Omega/\square$.

Summary

An analytical model for the collector current in Si/Si_{1-x}Ge_x/Si npn HBT's with graded bases has been presented, and shown to correspond well to actual devices. The experimental devices have near-ideal base currents, and low temperature current gains as large as 4000 have been observed.

Acknowledgements

The support of ONR (N00014-J-1316), NSF, and IBM is gratefully appreciated. The authors would also like to thank P.V. Schwartz and H. Manoharan for assistance in the material growth and characterization, and C. King for providing the masks used in this work.

References

1. G.L. Patton et al., IEEE Electron Dev. Lett., vol. 11, pp. 171-173, 1990.
2. C.A. King, J.L. Hoyt, and J.F. Gibbons, IEEE Trans. Electron Devices, vol. 36, pp. 2093-2104, 1989.
3. H. Kroemer, Solid State Electronics, vol. 28, pp. 1101-1103, 1985.
4. J.F. Gibbons, C.M. Gronet, and K.E. Williams, Appl. Phys. Lett., vol. 47, pp. 721-723, 1985.
5. R. People and J.C. Bean, Appl. Phys. Lett., vol. 48, pp. 538-540, 1986.

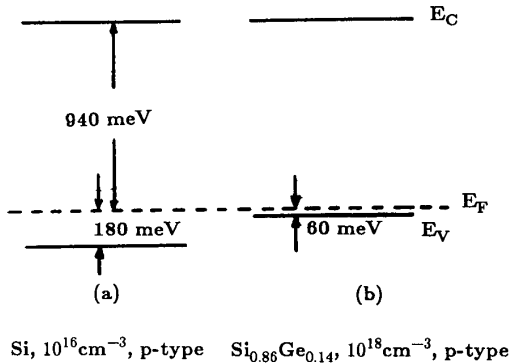


Fig. 1. Position of valence and conduction bands for constant Fermi level. The conduction band energy seen by electrons for (a) p-type Si doped 10^{16} cm^{-3} , and (b) $\text{Si}_{0.84}\text{Ge}_{0.16}$ doped 10^{18} cm^{-3} is the same in both cases.

device #	% Ge at base-emitter junction	$\Delta E_{G,1}$ (meV)	% Ge at base-collector junction	$\Delta E_{G,2}$ (meV)
1	0	0	20	168
2	7	50	20	168
3	13	100	20	168
4	20	168	20	168
5	0	0	0	0

Fig. 3. Layers grown by rapid thermal chemical vapor deposition for HBT's. The Ge concentration in the base varies linearly across the base.

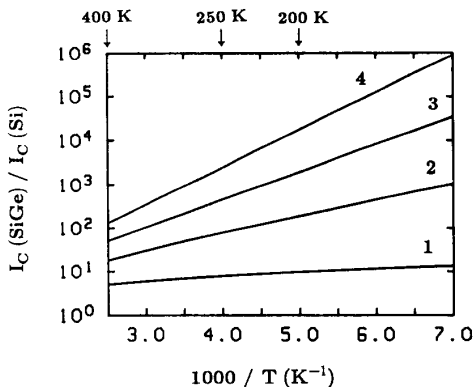


Fig. 4. Collector current divided by that of an all silicon device with the same actual total integrated base dopant, for device structures #1 - 4 as predicted by (1).

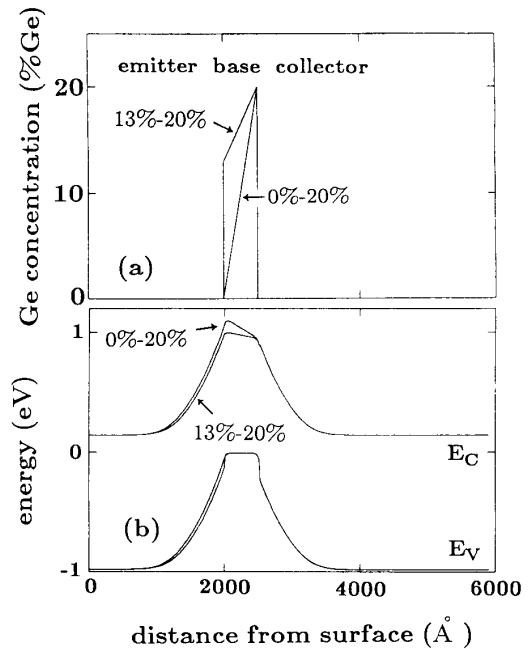


Fig. 2. (a) Ge concentration vs. distance for HBT's with graded bases, and (b) the resulting band diagrams for these devices with no applied bias. Note the accelerating electric field for electrons in the base, and the higher barrier in the conduction band in the device with less germanium.

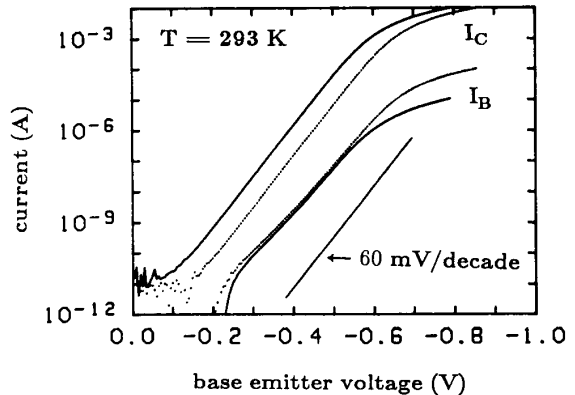


Fig. 5. Room temperature Gummel plots for device #3 (13-20% Ge, solid line) and for device #2 (7-20% Ge, dotted line). Note the increased collector current for the device with a larger $\Delta E_{G,1}$ (i.e. smaller conduction band barrier).

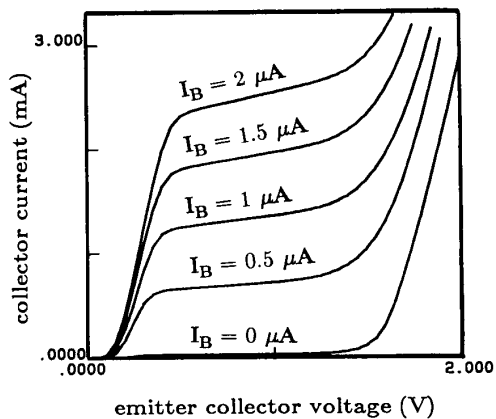


Fig. 6. Common-emitter characteristics of device #3 (13-20% Ge).

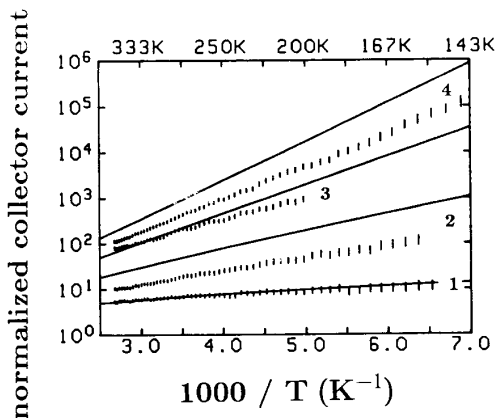


Fig. 7. Measured collector current enhancement for devices #1 - 4 (compared to all-silicon device #5) vs. inverse temperature, and comparison with the model of eqn. (1).

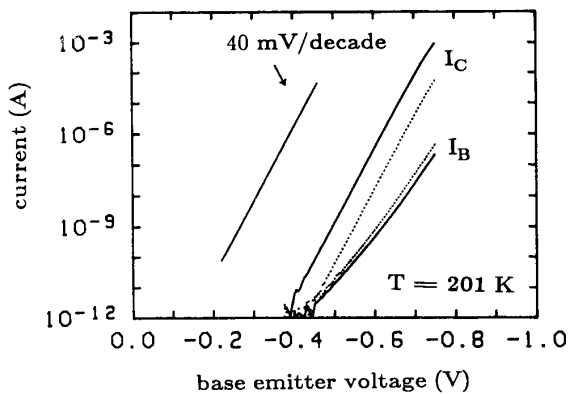


Fig. 8. Low-temperature (201 K) Gummel plots for device #3 (13-20% Ge, solid line) and device #2 (7-20% Ge, dotted line). The current gains at high current levels are larger than those at room temperature (fig. 5).

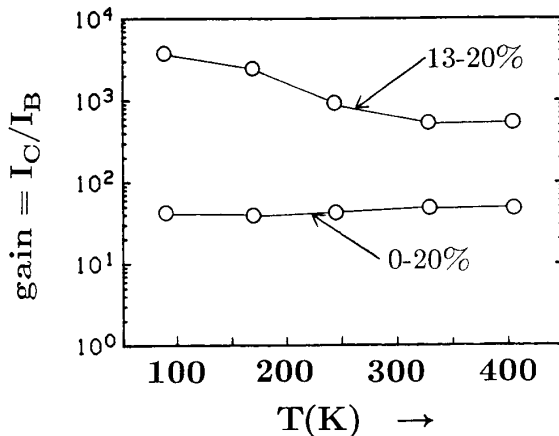


Fig. 9. Current gain vs. temperature for two different graded base devices.

2.2.4